Eur. Phys. J. B **32**, 437–444 (2003)
DOI: 10.1140/epjb/e2003-00125-4

THE EUROPEAN PHYSICAL JOURNAL B

Observation of a sharp lambda peak in the third harmonic voltage response of high-T_c superconductor thin films*

N. Chéenne[1], T. Mishonov[1,2], and J.O. Indekeu[1,a]

[1] Laboratorium voor Vaste-Stoffysica en Magnetisme, Katholieke Universiteit Leuven, Celestijnenlaan 200 D, B-3001 Leuven, Belgium
[2] Department of Theoretical Physics, Sofia University St. Kliment Ohridski, 5 J. Bourchier Blvd., 1164 Sofia, Bulgaria

Received 13 November 2002 / Received in final form 21 February 2003
Published online 7 May 2003 –

Abstract. In this paper, we report on the sharp peak observed in the third harmonic voltage response generated by a bias sinusoidal current applied to several strips patterned in a $YBa_2Cu_3O_{7-\delta}$ thin film and in two $La_{2-x}Sr_xCuO_4$ thin films, when the temperature is close to the normal-superconductor transition. The lambda-shaped temperature dependence of the third harmonic signal on the current characteristics is studied. Several physical mechanisms of third harmonic generation are examined.

PACS. 74.25.Fy Transport properties (electric and thermal conductivity, thermoelectric effects, etc.)

1 Introduction

Harmonic signals created by ac excitation have been used for a long time in the investigation of high temperature superconductors (HTSC) [1]. Particularly, a third harmonic signal is a consequence of non-linear effects and its measurement is a powerful technique to investigate, and moreover, to discriminate between the different possible origins of these non-linearities. Different techniques of third harmonic measurement exist for investigating properties of HTSC devices especially in microwave range [2–6], or for characterizing material properties such as thermal conductivity [7–11], specific heat [11], current response [12], or critical temperature [13].

The existence of a sharp maximum in the third harmonic can be easily understood from a qualitative point of view. At low temperatures the voltage response of the superconducting phase is almost zero. On the other hand, in the normal phase we have with high accuracy an ohmic behaviour and the response at higher frequency harmonics is again small. A sharp maximum related to a viable variety of nonlinear phenomena is expected only close to the critical temperature.

As an example, measurement of the third harmonic of the ac susceptibility revealed the role of interplanar spacing on formation of flux lines and demonstrated that the irreversibility field in Bi2212 is determined by surface barriers [13,14]. This is related to vortex motion, which is one of the possible origins of the non-linear effects in electrical properties in HTSC [15]. See also references [16] and [17] where a mechanism is discussed for the generation of third harmonics based on the anisotropic scattering rate of normal charge carriers included in the Boltzmann equation.

One of the other possible roots of this non-linear behaviour is given in reference [18], where a theoretical derivation is presented to explain non-linear effects in electrical conductivity close to the transition temperature. From this paper [18], it is expected that the measurement of the third harmonic voltage allows getting hold of superconductor constants of the BCS theory. In addition, the authors [18,19], investigate theoretically the third harmonic voltage generation produced by the thermal response of the film to a harmonic current. Third harmonic response is definitely related to different roots of non-linear effects and should allow one to gather new information about the mechanism of HTSC non-linearity.

In the present paper, systematic measurements of the voltage response to a harmonic current across HTSC strips patterned in a $YBa_2Cu_3O_{7-\delta}$ (YBCO) thin film and in two $La_{2-x}Sr_xCuO_4$ (LSCO) thin films with $x = 0.15$ were performed as a function of temperature. First and third harmonics were recorded for the whole temperature range, from room temperature to a few kelvin below the normal-superconductor transition. A sharp peak was observed in the third harmonic voltage close to the critical temperature, exhibiting a lambda-shaped (λ-shaped) behaviour. This λ-shaped peak was investigated for different current amplitudes and frequencies.

* Grants: This research has been supported by the Belgian DWTC, IUAP, the Flemish GOA and VIS/97/01 Programmes. T.M. is KUL Senior Fellow (F/00/038) and N.Ch. is supported by the EC TMR Network Contract nr. ERB-FMRX-CT-980171 and by the Flemish FWO project G.0222.02

[a] e-mail: joseph.indekeu@fys.kuleuven.ac.be

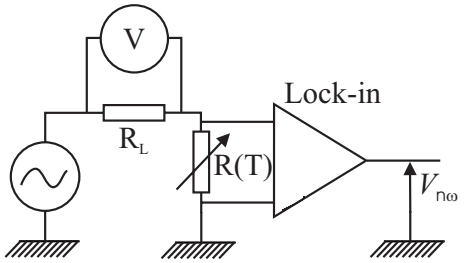

Fig. 1. Scheme of the electrical measurements. The current in the superconductor sample (symbolized by its temperature-dependent resistance $R(T)$) is governed by the voltage generator and the load resistance R_L. The voltmeter across R_L allows to monitor the current in the sample. The rms voltage harmonic response ($V_{n\omega} \div \sqrt{2}$, $n = 1, 3$) across the sample is measured by a lock-in amplifier and recorded as a function of temperature.

Sample and measurement descriptions are given in Section 2 of this paper. Complete experimental data processing and observations are presented in Section 3. In Section 4, mechanisms of third harmonic signal generation are briefly discussed.

2 Experimental setup

Measurements were first performed on two different strips designed in a YBCO thin film, 180 nm thick, deposited by DC sputtering on a MgO substrate, as described in [20] and [21]. The smallest is 1.59 mm long and 77 μm wide, and the largest is 2.87 mm long and 474 μm wide. Both were chemically etched in acid solution. A second set of measurements was performed on 1 mm long and 100 μm wide strips patterned on two different LSCO films, LSCO1 and LSCO2, both deposited by sputtering on a $SrTiO_3$ substrate. The first one was synthesized at 850 °C, under 1.83 mbar of pure oxygen, and annealed under pure oxygen at 10 mbar at 850 °C for half an hour. For the second one, the temperature of deposition and annealing was decreased to 840 °C.

The samples were placed in a cryostat and exposed to a helium flux. The connection between the electronic equipment and the strip was made *via* coaxial cables in a four-points geometry (Fig. 1). Strips were bias current, the latter being sinusoidal with amplitude I_0 and frequency $f = \omega/2\pi$. The rms current value $I_0/\sqrt{2}$ was monitored during the whole experiment by measuring the voltage across the load resistance R_L, chosen large enough to have negligible variation of the current (less than 10 %). Using a digital lock-in amplifier (model SR830 from Stanford Research Systems), first ($V_{1\omega}$) and third ($V_{3\omega}$) harmonics of the voltage developed in the sample were successively recorded simultaneously with temperature and time.

As was mentioned in previous papers [7,19], the current has to be much smaller than a maximal value I_G to be far from thermal runaway conditions:

$$I_G = \sqrt{\frac{G}{|R'|}}, \tag{1}$$

where R' is the first derivative of the electrical resistance with respect to temperature and G is the thermal boundary conductance between the strip and the substrate, which is maintained at the temperature of the helium bath. The sample is in contact with stationary (non-flowing) helium gas. At low temperature-scanning velocities (typically 1 K/min) the contact gas is in thermal equilibrium with the sample so that convection losses at the gas-sample interface are minimal. G can be expressed through the thermal boundary conductivity g, the length L and the width w of the strip:

$$G = gLw. \tag{2}$$

In the case of the YBCO film, calculating I_G from standard values of g (2000 W/Kcm^2) and R' (1 Ω/K) in the normal state, we found the maximal current to equal 1.6 A for the narrowest strip and 5.2 A for the widest one. In our case, the maximum current used had an amplitude of 7 mA, far enough from the limit given by equation (1). Concerning the LSCO films, the biggest current amplitude used was 1.4 mA, while the estimated I_G is 1.4 A using the same (order-of-magnitude) estimates for g and R' as for YBCO.

3 Experimental observations

3.1 Experimental data processing

Before showing our results, we explain in some detail the experimental data processing, taking as an example the measurements obtained from the YBCO film. The goal of this processing is to calculate the first and the second derivatives of the resistance with respect to temperature, which we need to estimate the thermal conductance G, as described in reference [19]. Since our cryogenic system induces strong temperature fluctuations, temperature data were smoothed over time, using a Savitzky-Golay filter [22], which performs a local polynomial regression to determine the smoothed value for each data point. In our case, 2nd order polynomial regression was used, taking into account 25 points to the left and 25 points to the right.

The same smoothing was used to filter the electrical resistance of the strip, R. Since the frequency ω is in the kHz range, we consider the superconducting strip as a purely ohmic device where inductive and capacitive components are negligible. The resistance is then deduced from $V_{1\omega}$ by Ohm's law:

$$R_{1\omega} = \frac{V_{1\omega}}{I_0}. \tag{3}$$

In this case, only 5 points to the left and 5 points to the right were taken into account to perform the local regression, to avoid any big distortion close to the superconducting transition. Exactly the same procedure was applied for smoothing the third harmonic voltage.

Thus, sets of time-dependent smoothed-data were obtained and used to calculate the first and second derivatives of the temperature ($\dot{T}$, $\ddot{T}$) and resistance ($\dot{R}$, $\ddot{R}$) with

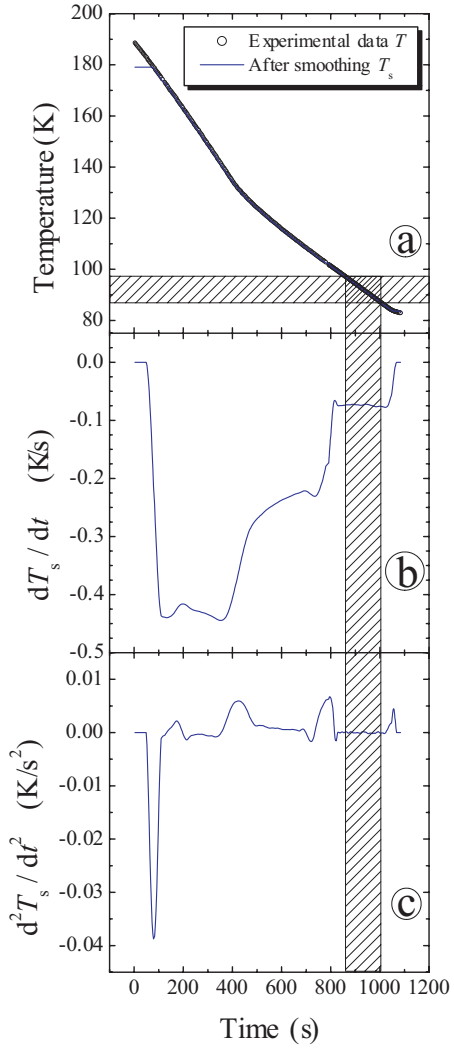

Fig. 2. Recording of temperature T *vs.* time (a), and first (b) and second (c) derivatives of its smoothed values T_s.

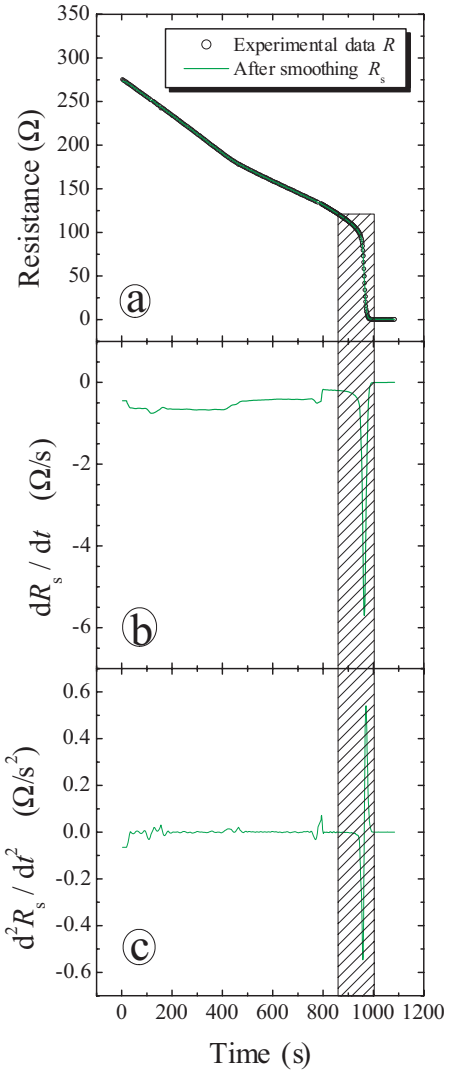

Fig. 3. Recording of resistance R *vs.* time (a), and first (b) and second (c) derivatives of its smoothed values R_s.

respect to time t, differentiating using Savitzky-Golay smoothing. For this step, the local smoothing was performed on the smoothed-data sets. The local regression taking into account 21 points for the temperature set and 11 points for the resistance set, allowed to deduce the first and the second derivatives for each data point. Thus, it was straightforward to determine for each point in time, the values of the first and second derivatives of the resistance with respect to temperature T:

$$R'(T) = \frac{\dot{R}}{\dot{T}}, \qquad R''(T) = \frac{\ddot{R}\dot{T} - \dot{R}\ddot{T}}{(\dot{T})^3}, \tag{4}$$

All the steps of the experimental data processing are gathered in Figures 2 and 3, presenting, respectively, the temperature, the resistance and their respective derivatives obtained for the narrowest strip excited by a current of 4 mA rms. The temperature was shifted by a few kelvin during the measurements due to the poor thermal conductivity of the sample holder on which our temperature diode and sample were glued; we then shifted all temperature data sets by 4 K in order to have a reasonable T_c of 90 K for our YBCO sample.

Figures 4 and 5 give the resistance and its first and second derivatives with respect to smoothed temperature, deduced from the time-dependent data sets shown in Figures 2 and 3, with use of equation (4). These results were used to calculate the thermal conductance G between the strip and the heat sink, as described in [19] and to evaluate the contribution of the thermal effect in the peak observed in the third harmonic voltage $V_{3\omega}$, which will be described in the next section.

3.2 Lambda shape of the 3rd harmonic voltage $V_{3\omega}$

Figure 6 gives the temperature dependence of the third harmonic response of the narrowest strip patterned on the YBCO film to a current excitation equal to 4 mA rms and a modulation frequency of 1024 Hz.

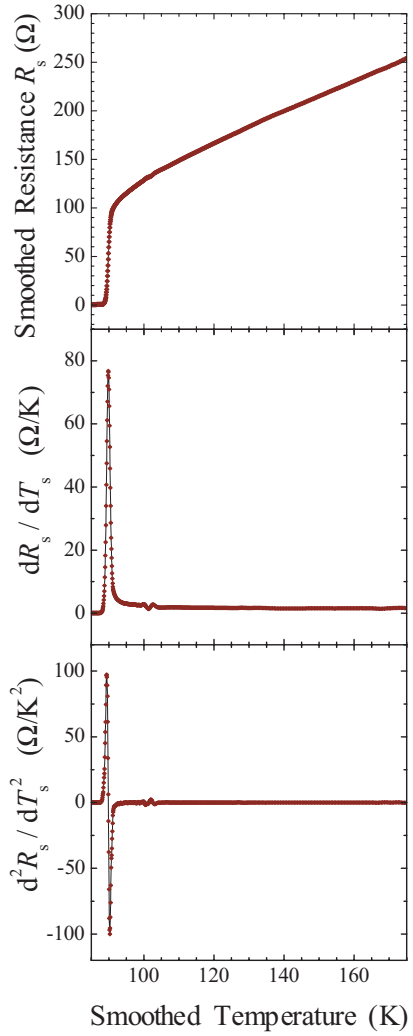

Fig. 4. The resistance and its first and second derivatives with respect to temperature deduced from equation (4) and data sets extracted from Figures 2 and 3.

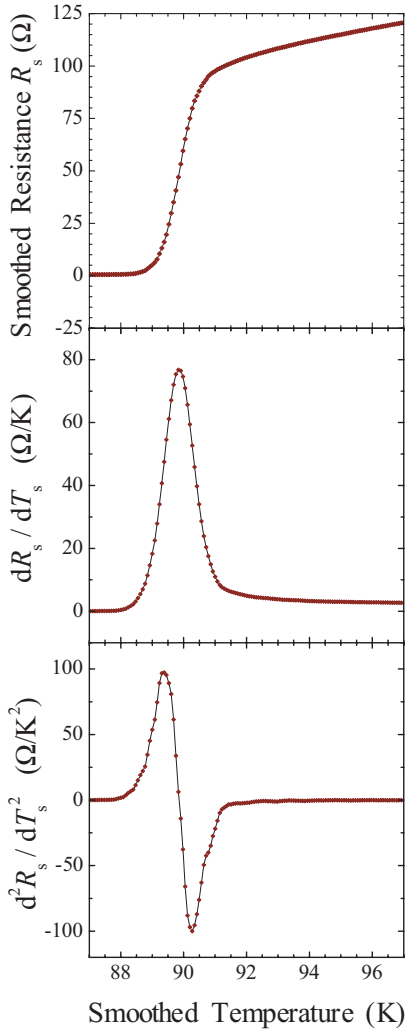

Fig. 5. The resistance and its first and second derivative with respect to temperature, on the temperature range indicated by the hatched areas in Figures 2 and 3.

To have an appreciation of the common behaviour of the third harmonic response for different samples, we performed the same kind of measurement on two LSCO films. Figures 7 and 8 present for each tested sample (LSCO1 and LSCO2) both the resistance and the third harmonic response obtained for currents ranging from 10 μ A rms to about 1 mA rms, as a function of the temperature. The sharp transition of the resistance presented in Figure 7a gives rise to a unique lambda-shaped peak in Figure 7b. In the case of a sample exhibiting a "double" transition in the resistivity as for LSCO2 (see Fig. 8a), we observe two peaks in the third harmonic voltage response, Figure 8b. This puts into evidence the high accuracy of this technique of measurement, firstly, to determine the critical temperature of a material in a very simple way, and further, to differentiate between different phases in a material and to give for each of them the critical temperature.

The behaviour of the shape and the amplitude of the peak with respect to current characteristics has been explored. As we can see in Figures 7b and 8b the amplitude

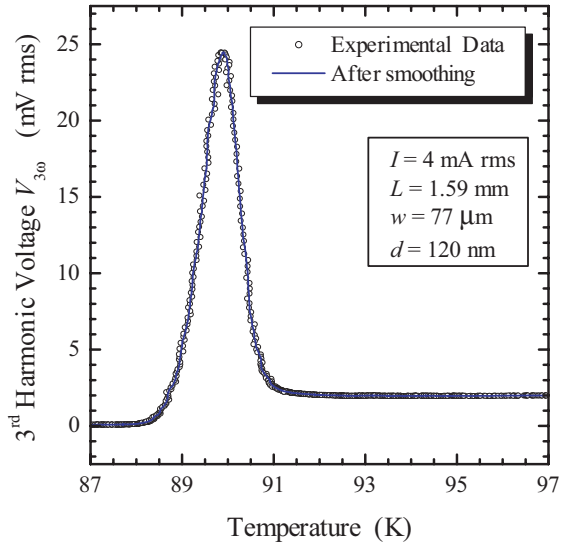

Fig. 6. λ-shaped temperature dependence of the third harmonic voltage $V_{3\omega}$ for YBCO.

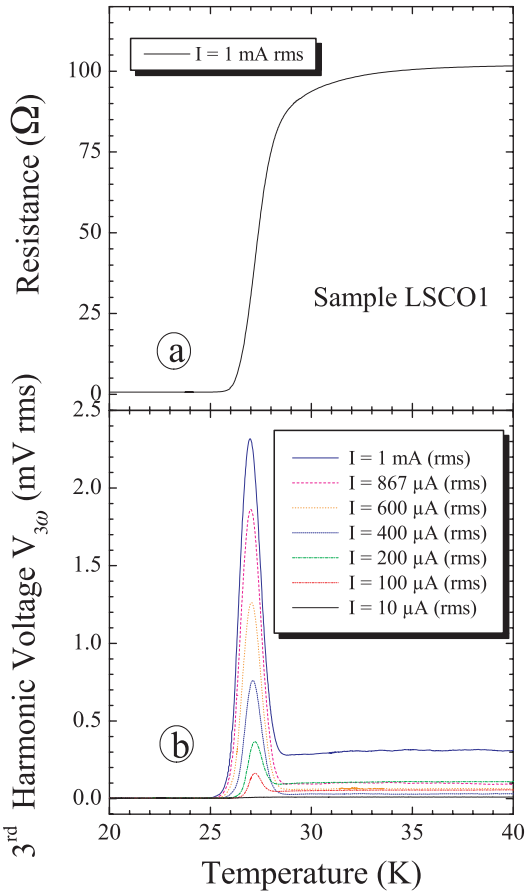

Fig. 7. Measurements on LSCO1. (a): Dependence of the strip resistance on temperature; (b): Dependence of the third harmonic signal on temperature for different current amplitudes.

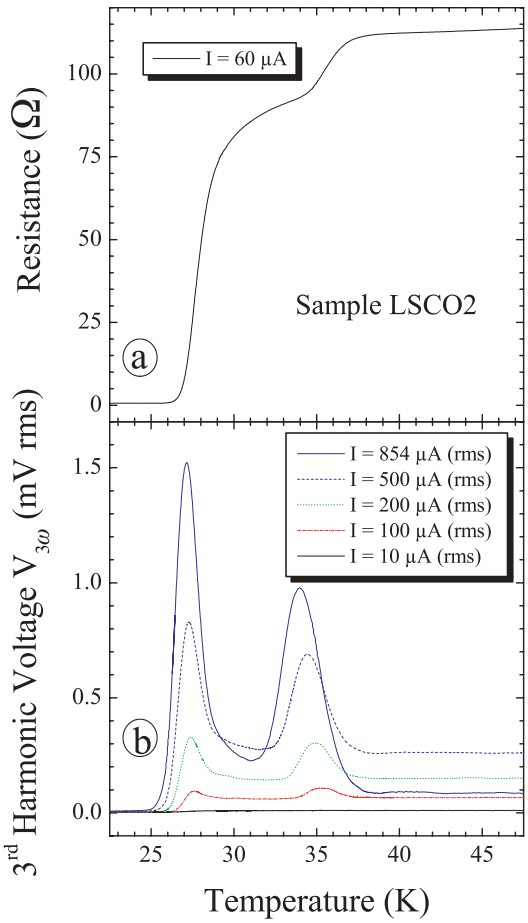

Fig. 8. Measurements on LSCO2. (a): Dependence of the strip resistance on temperature; (b): Dependence of the third harmonic signal on temperature for different current amplitudes.

of the peak increases with the current. Figure 9 presents the dependence of the peak value of the third harmonic response on the current amplitude in a log-log plot. A power law dependence of the third harmonic peak amplitude on the current intensity is exhibited for each curve. But no clear power law emerges, the power ranging from 1.1 for the LSCO1 film to 3/2 for the YBCO film. We are also not aware of a theoretical prediction of a power law for the peak amplitude versus current. At T_c, various contributions to the third harmonic play a role and are difficult to estimate.

For $T > T_c$, the situation is easier to analyse theoretically [18,19] and a power law with an exponent 3 is predicted for the dependence of the third harmonic amplitude on the current. In our experiments, however, a complication arises due to the presence of a parasite current coming from our generator, $I_{3\omega}$, which produces a third harmonic signal that plays an important role in this temperature range. This effect hides the real amplitude of the third harmonic signal. Following the theoretical works [18,19], we have adopted a fitting procedure which takes into account this parasite current. In any case, even with these difficulties, it is important to note that the third harmonic signal presented in this paper follows qualitatively the expected lambda-shaped behaviour predicted in [19].

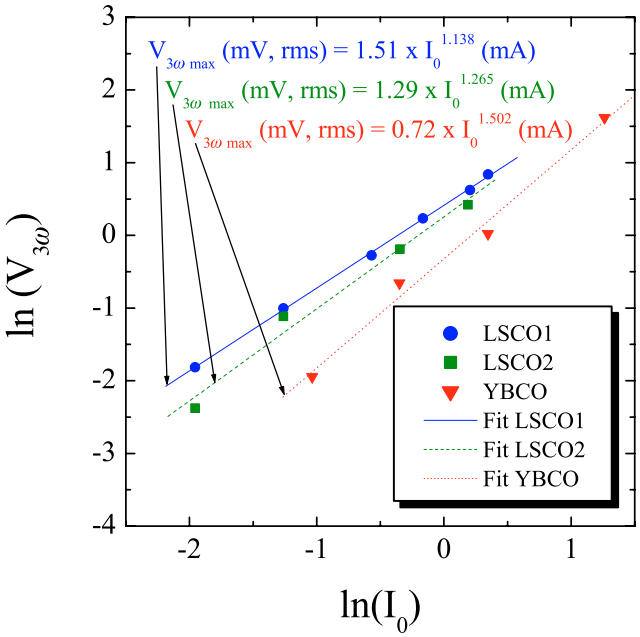

Fig. 9. Dependence of the maximum of the third harmonic signal on current amplitudes for the three tested samples.

3.3 Experimental data analysis

Figure 10 presents the first attempt to connect theory and experiment. It shows the fit of the lambda shape, in the case of the 1 mA rms current excitation, using two different functions. The first one takes into account only the thermal effect. In the second one, both the thermal effect and the nonlinear current generated by the generator, $I_{3\omega}$, are considered.

To have an appreciation of the reliability of the fit, the thermal resistivity r_h between the film and the heat sink has been calculated from the thermal resistance R_h given by the fit, considering the surface of the patterned strip (100 μm $\times$ 1 mm). If we consider the case where both the parasitic current $I_{3\omega}$ and the thermal conductance effects are present, the fit gives a value of R_h equal to 580 K/W, which corresponds to a thermal resistivity equal to 5.8×10^{-5} m^{2}K/W at the considered temperature (about 30 K). To our knowledge, no data has been published concerning the thermal boundary resistivity of LSCO thin films at this temperature. Then we compare the obtained value to the one theoretically predicted in [23] for a YBCO thin film deposited on MgO. The value predicted in the latter [23] is about 10^{-6} m^{2}K/W at 30 K. Our experimental value is not far from this theoretically predicted value (about one order of magnitude bigger). Because the nature of substrate and film are different, some difference is to be expected. Furthermore, in the range of temperatures considered (20 K $\leq$ T $\leq$ 60 K), the variation of the thermal boundary resistivity is rather large.

The dependence of the peak on the current frequency was studied at fixed amplitude current (I_0 = 1.41 mA). No differences in the peak were observed for frequencies ranging from 114 Hz to 20.6 kHz.

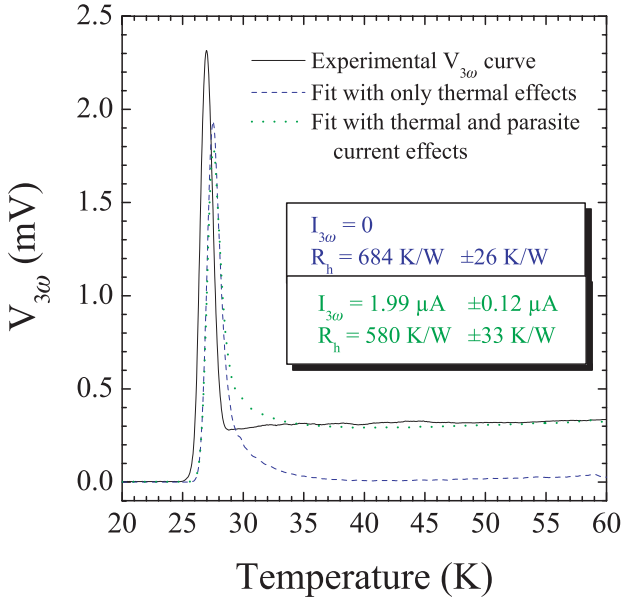

Fig. 10. Fit of the lambda-shaped peak in the case of a 1 mA rms current measurement on LSCO1, taking into account the thermal effect only (with the thermal resistance R_h between film and substrate as parameter), or both the thermal and the parasite $I_{3\omega}$ current effects. The equation used for the fitting procedure is: $V_{3\omega} = RI_{3\omega} + \frac{R_h R R' I_0^3}{4} + \frac{5R_h^2 R(2R'^2 + RR'')I_0^5}{32}$.

4 Discussion and conclusion

The main qualitative property of the third harmonic response is the sharp λ-peak close to the critical temperature. Taking into account the third harmonic signal generated by the thermal oscillations in the film and by the parasite current from the generator, the experimental data have been fitted. From this procedure, we found an acceptable value of the thermal resistivity, r_h, and a reasonable value of the parasite current, $I_{3\omega}$. Thus, we have for the moment a qualitative agreement between experiments and theory.

A more detailed investigation, beyond the partial analysis presented in Section 3.3, of the dependence of the height and width of this peak on the current and geometry of the strip (especially the thickness) will be the theme of further research. This should be helpful to discriminate the different contributions to the third harmonic response above T_c, close to the critical temperature, *i.e.* the thermal oscillation part and the non-linear conductivity part.

Other third harmonic sources (including the non-linear conductivity) would have to be taken into account to describe more accurately the whole peak. For example, a temperature shift of the peak is not yet explained by the proposed theories [18,19]. Also, slightly above T_c, we observe a disagreement between our fit and the experimental data in the tail of the peak. Let us discuss in brief some mechanisms for the generation of harmonics in different temperature regimes and physical situations, which would have to be taken into account to describe the whole peak with a better accuracy.

At very low temperature, in the vortex pinning regime or in a vortex-free situation, modulation of the superconducting order parameter creates dissipation and harmonic generation [24,25]; the non-linearity is created by the current dependence of the superfluid density which can be easily described within the Ginzburg-Landau model [26]. Non-linear response of the vortex state [15] can also create higher harmonics. However, the complexity of the pinning mechanisms and the generation of a magnetic field by the applied current makes it very difficult to develop a detailed theory for the low-temperature tail of the λ-shaped maximum. For example, small superconducting grains in a diamond anvil [13,14], or scanning of the surface of a thin film by a terminated coaxial cable [4] require the solution of different electrodynamics problems. In our paper, we used a narrow strip and the vortices are created near the edges of the sample by the applied current. The generation of vortices can be significantly reduced if a Corbino geometry is used; it is necessary that a superconducting film terminates a coaxial cable.

For temperatures slightly above the critical one, there is significant fluctuation conductivity. Usual ohmic

conductivity of normal carriers is perfectly linear but fluctuation conductivity is not and can create an observable part of the harmonic generation [18].

For higher temperatures, temperature oscillations can create harmonics in the voltage response [7,8,19,27]. It is this mechanism which has been given most attention in our theoretical analysis of the experimental data for $T > T_c$ (see Fig. 10).

For completeness, we would like to mention that analogously to temperature oscillations well above T_c, a quite universal mechanism for 3rd harmonic generation at microwave frequencies exists for the superconducting state below T_c. The density of superfluid particles depends on the applied current and finally the kinetic inductance of the superconducting sample depends on the current $I = I_0 \cos(\omega t)$

$$L(I) \approx L_0 + L_1 I^2. \tag{5}$$

L_0 gives the linear contribution to the kinetic inductance and L_1 the non-linear one (see Refs. [24,25]). Then, the general formula for the voltage response given by

$$V(t) = L(I)\frac{\mathrm{d}I}{\mathrm{d}t} \tag{6}$$

allows to calculate the third harmonic response [24,25]:

$$V_{3\omega} = -\frac{L_1 \omega I_0^3}{4}\sin(3\omega t). \tag{7}$$

It appears in this formula that the third harmonic response increases linearly with the frequency. This explains that it is typically observed in the microwave range devices. In our range of frequencies (up to 20 kHz), this response is not expected to be observable.

Apart from studying the interface heat resistance, for the fundamental physics of superconductivity of layered cuprates it will be very interesting to investigate the bulk non-ohmic conductivity related to the kinetics of the normal phase. For further theoretical discussion see for example [16,17] and [28].

In conclusion, the investigation of the λ-peak of the third harmonic response is a good qualitative method for the detection of the superconducting phase transition. Because of the simplicity of the measurement, it can become a standard method in the materials science of superconductors and also in the industry for testing the quality of the thin films and cables. In order to separate the bulk and interface mechanisms for the third harmonic generation it is necessary to perform detailed investigations of superconducting films with different thicknesses. In this way applied research related to the development of superconducting bolometers can become an indispensable tool for the investigation of the fundamental effects in cuprate superconductors [29,30]. Our work demonstrates that the maximum of the λ-shaped peak as a function of temperature can be very easily observed, even without any special care for signal cleaning.

Because the voltage generator produces some third harmonic signal, if we wish to investigate the third harmonic far from T_c, we have to compensate the parasite 3ω-signal not only at the level of the data analysis, but also electronically. However, a very simple filter will lead to a reduction of the ratio $I_{3\omega}/I_0$ ($\approx 1/500$) by a factor of about 10 only, so that the remaining parasite contribution must still be taken into account in the data analysis, as described in the theoretical works (Eqs. (7.10) from [18] and (3.8) from [19]).

Detailed investigation of the third harmonic response provides a reliable method for the investigation of superconductor thermal properties like thermal conductivity, thermal boundary resistance and heat capacity. Moreover, if the thermal effects are carefully subtracted, the investigation of the third harmonic signal will provide the opportunity to extract the relaxation time of the superconducting order parameter from the isothermal electric non-linearity. If a Corbino geometry does not create significant heating of the sample, this can be expected to be the best experimental setup for the observation of Cooper-pair depairing non-linearity.

Special thanks goes to Patrick Wagner [20] and Johan Vanacken who provided us with YBCO and LSCO thin films. Also we would like to express our gratitude to Johan Vanacken for assistance with the experiments, and to Gunther Rens for Atomic Force Microscopy characterisation of the film thickness. T.M. would like to thank Valya Mishonova for bringing reference [27] to his attention and Richard Hlubina and Didier Robbes for their correspondence.

References

1. L. Ji, R.H. Sohn, G.C. Spalding, C.J. Lobb, M. Tinkham, Phys. Rev. B **40**, 10936 (1989); and references [2–6] therein
2. M.R. Trunin, G.I. Leviev, J. Phys. III France **2**, 355 (1992)
3. A. Agliolo Gallitto, M. Li Vigni, Physica C **305**, 75 (1998)
4. E.E. Pestov, Y.N. Nozdrin, V.V. Kurin, *Third-order local nonlinear microwave response of $YBa_2Cu_3O_7$ and Nb thin films, ASC2000, Virginia Beach, Virginia, 17-22 Sept. 2000*, published in IEEE Trans. Appl. Supercond. **11**, 131 (2001), E.E. Pestov, Y.N. Nozdrin, V.V. Kurin, *A new method for a local study of nonlinear microwave properties of superconductors*, `cond-mat/0005501`. In this paper are discussed some mechanisms of surface resistance nonlinearity. In reference [2] of this paper, a correlation was found between the depinning current density and the nonlinear microwave response
5. J.C. Booth, J.A. Beall, R.H. Ono, F.J.B. Stork, D.A. Rudman, L.R. Vale, IEEE Trans. Appl. Supercond. **5**, 2652 (1995)
6. H. Shimakage, J.C. Booth, L.R. Vale, R.H. Ono, Supercond. Science Techn. **12**, 830 (1999)
7. D. Robbes, N. Chéenne, J.F. Hamet, J.P. Rice, IEEE Trans. Appl. Supercond. **9**, 3874 (1999). In equation (1) of this paper, I_0^3 is misprinted as I_0^2, *cf.* next reference [8]
8. N. Chéenne, *Synthèse de films minces de type superréseau pour la réalisation et l'étude de micro-bolomètres. Rôle des interfaces sur la transmission des phonons (The study and design of multilayered microbolometers, and the role of the interfaces on the reflection of phonons)*, Ph.D. Thesis, University of Caen, France (Dec. 2000) p. 127, Eq. (III-46) (in French, unpublished); n° 06002898X

9. D.G. Cahill, Rev. Sci. Instrum. **61**, 802 (1990)
10. T. Borca-Tasciuc, A.R. Kumar, G. Chen, Rev. Sci. Instrum. **72**, 2139 (2001)
11. L. Lu, W. Yi, D.L. Zhang, Rev. Sci. Instrum. **72**, 2996 (2001); references therein, especially the historical paper on thermal information extracted from ac heating (O.M. Corbino, Phys. Z. **11**, 413 (1910))
12. T. Dahm, D.J. Scalapino, Phys. Rev. B **60**, 13125 (1999), preprint `cond-mat/9908332`
13. M.P. Raphael, M.E. Reeves, E.F. Skelton, Rev. Sci. Instrum. **69**, 1451 (1998)
14. M.P. Raphael, M.E. Reeves, E.F. Skelton, C. Kendziora, Phys. Rev. Lett. **84**, 1587 (2000), preprint `cond-mat/9908156`
15. R. Mallozzi, J. Orenstein, J.N. Eckstein, I. Bozovic, Phys. Rev. Lett. **81**, 1485 (1998)
16. R. Hlubina, Physica C **319**, 159 (1999)
17. K.G. Sandeman, A.J. Schofield, Phys. Rev. B **63**, 094510 (2001), `preprint cond-mat/0007299`
18. T. Mishonov, A. Posazhennikova, J. Indekeu, Phys. Rev. B **65**, 064519 (2002), `cond-mat/0106168`
19. T. Mishonov, N. Chéenne, D. Robbes, J. Indekeu, Eur. Phys. J. B **26**, 291 (2002), `cond-mat/0109478`
20. P. Wagner, F. Hilmer, U. Frey, H. Adrian, T. Steinborn, L. Ranno, A. Elschner, I. Heyvaert, Y. Bruynseraede, Physica C **215**, 123 (1993)
21. B. Wuyts, Z.X. Gao, S. Libbrecht, M. Maenhoudt, E. Osquiguil, Y. Bruynseraede, Physica C **203**, 235 (1992)
22. W.H. Press, S.A. Teukolsky, W.T. Vetterling, B.P. Flannery, *Numerical Recipes in Fortran 77: The art of scientific computing*, Vol. 1 of *Fortran Numerical Recipes* (Cambridge University Press, Cambridge, 2001); Fig. 14.8.2-1, p. 644–649; Software Product Origin
23. P.E. Phelan, J. Heat Transfer **120**, 37 (1998)
24. J.C. Booth, J.A. Beall, D.A. Rudman, L.R. Vale, R.H. Ono, J. Appl. Phys. **86**, 1020 (1999)
25. J.C. Booth, L.R. Vale, R.H. Ono, J.H. Claassen, J. Supercond.: Incorp. Novel Magnetism **14**, 65 (2001)
26. E.S. Borovitskaya, V.M. Leviev, G.I. Genkin, JETP **83**, 597 (1996)
27. A.A. Zharov, A.L. Korotkov, A.N. Reznik, Supercond. **5**, 413 (1992); A.A. Zharov, A.L. Korotkov, A.N. Reznik, Supercond. Sci. Technol. **5**, 104 (1992); and reference [6] therein: Richards P.L. *et al.*, *Ext. Abstr. 3rd Int. Superconductive Electronics Conf. 25-27 June 1991, University of Stratchclyde, Glasgow, Scotland, p. 15*; see also P.L. Richards, J. Appl. Phys. **76**, 1 (1994); A.L. Korotkov, A.N. Reznik, A.A. Zharov, Supercond. Sci. Technol. **9**, 353 (1996)
28. R. Hlubina, T.M. Rice, Phys. Rev. B **51**, 9253 (1995), preprint `cond-mat/9501086`; R. Hlubina, T.M. Rice, Phys. Rev. B **52**, 13043E (1995); R. Hlubina, Phys. Rev. B **58**, 8240 (1998)
29. J.M. Gildemeister, A.T. Lee, P.L. Richards, Appl. Phys. Lett. **74**, 868 (1999)
30. J.M. Gildemeister, A.T. Lee, P.L. Richards, Appl. Phys. Lett. **77**, 4040 (2000)